

OPEN ACCESS

Quantum Networks with Atoms and Photons

To cite this article: C Monroe *et al* 2013 *J. Phys.: Conf. Ser.* **467** 012008

View the [article online](#) for updates and enhancements.

Related content

- [Phase control of trapped ion quantum gates](#)
P J Lee, K-A Brickman, L Deslauriers *et al.*
- [Quantum simulation of the transverse Ising model with trapped ions](#)
K Kim, S Korenblit, R Islam *et al.*
- [Phonon-mediated entanglement for trapped ion quantum computing](#)
K-A Brickman Soderberg and C Monroe

Recent citations

- [Non-thermalization in trapped atomic ion spin chains](#)
P. W. Hess *et al*

Quantum Networks with Atoms and Photons

C. Monroe¹, W. Campbell², C. Cao¹, T. Choi¹, S. Clark¹, S. Debnath¹, C. Figgatt¹, D. Hayes, D. Hucul¹, V. Inlek¹, R. Islam¹, S. Korenblit¹, K. Johnson¹, A. Manning¹, J. Mizrahi¹, B. Neyenhuis¹, A. Lee¹, P. Richerme¹, C. Senko¹, J. Smith¹, and K. Wright¹

¹ Joint Quantum Institute, University of Maryland Department of Physics and National Institute of Standards and Technology, College Park, MD 20742

² Department of Physics and Astronomy, University of California Los Angeles, Los Angeles, CA 90095

E-mail: monroe@umd.edu

Abstract. Trapped atomic ions are standards for quantum information processing, as all of the fundamental quantum operations have been demonstrated in small collections of atoms. Current work is concentrated on scaling ion traps to larger numbers of interacting qubits and the generation of massive entangled states. We discuss progress in the quantum networking of trapped atomic ions, using the Coulomb interaction for demonstrations of simple quantum simulations of magnetism, ultrafast laser pulses for entanglement, and finally probabilistic photonic interactions to bridge entanglement over long distances.

Trapped atomic ions form ideal quantum systems for the fabrication of quantum information devices and the study of manybody quantum states. Trapped ion qubits enjoy an extreme level of isolation from the environment, they can be entangled through their local Coulomb interaction, and they can be measured with near-perfect efficiency with the availability of cyclic optical transitions [1]. Recent effort in this area has concentrated on the scaling to large numbers of trapped ion qubits, and there is continued progress on the use of monolithic chip traps and integrated optical interfaces for future ion-based quantum devices [2].

Here we highlight new directions in the quantum networking of trapped atomic ion systems undertaken by the JQI-Maryland Ion Trap Group. These efforts do not simply refine and improve earlier approaches of entanglement generation, but represent new methods for the generation of entangled networks with larger systems, at ultrafast times scales, and over macroscopic distances.

In all experiments, we confine atomic $^{171}\text{Yb}^+$ ions in linear radiofrequency (Paul) ion traps, and store effective spin- $1/2$ qubits in the $^2S_{1/2}$ ground state “clock” hyperfine levels, labeled by $|\uparrow\rangle$ ($F = 1, m_F = 0$) and $|\downarrow\rangle$ ($F = 0, m_F = 0$) and separated by a frequency of $\nu_0 = 12.64281$ GHz [3]. The qubits are initialized and detected with laser radiation near resonant with the $^2S_{1/2} - ^2P_{1/2}$ transition at a wavelength around 369.5 nm. We coherently couple the qubit levels via optical stimulated Raman transitions using off-resonant laser radiation. This interaction can be accompanied by optical dipole forces in certain applications.

Ultrafast Quantum Gates

The Raman laser for coherent operations on $^{171}\text{Yb}^+$ qubits is a mode-locked Nd:YVO₄ oscillator and amplifier that is frequency tripled to 355 nm. This wavelength is ideal for the $^{171}\text{Yb}^+$ system,



as its large detunings from the 2P states (33 THz blue of ${}^2P_{1/2}$ and 67 THz red of ${}^2P_{3/2}$) amount to negligible spontaneous emission and differential AC Stark shifts [4]. Furthermore, the large bandwidth of the pulses easily covers the hyperfine splitting, and the resulting frequency comb from a pulse train allows high resolution resolved-sideband control of trapped ion motion [5], similar to conventional setups involving cw lasers [6].

For higher Raman laser power, we have shown that a solitary pulse with a typical duration of about 10 ps can drive transitions between the two qubit states [4]. Such an interaction ushers a new regime of ultrafast atomic qubit control, and when applied to many trapped ions it has great promise for the operation of ultrafast entangling gates where the gate speed is faster than the period of harmonic trap motion [7, 8].

Toward this end, we apply counterpropagating pulses to the ions, with orthogonal linear polarizations. This creates a spatially modulated Rabi frequency that is the basis of a spin-dependent momentum kick [4]. We have verified the coherence of this process and resulting ultrafast qubit-motion entanglement by implementing a Ramsey interferometer with a single trapped ion. We first create a superposition of spin states with microwaves (first Ramsey $\pi/2$ pulse), then apply two ultrafast spin-dependent kicks with individual ultrafast laser pulses. After closing the interferometer (second Ramsey $\pi/2$ pulse), we expect fringes only when the kicks are separated by integral multiples of the trap period, because otherwise the momentum kicks are not parallel, and the motional wavepackets do not recombine. This periodic revival of qubit contrast is shown in Fig 1, showing the coherence of the kick process and the entanglement of spin and motion [9].

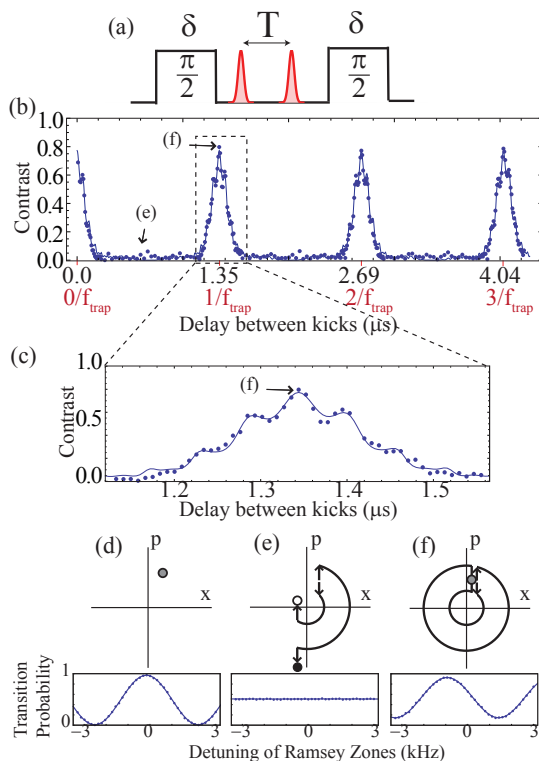


Figure 1. (a) Ramsey sequence for observation of ultrafast spin-dependent momentum kicks. A single trapped ion is driven by two microwave pulses detuned from resonance by δ , with two spin-dependent kicks in between. For each delay T between the kicks, δ is scanned and a Ramsey fringe contrast obtained. (b) Plot of the results of the experiment in (a).s At integer multiples of the trap period, contrast revives. (c) Close-up of the first revival peak in (b). The peak shape is a function of the thermal ion motion, and also residual micromotion that can be seen in the modulation of the revival peak. The best fit curve shown is a fit to theory with free parameters being the micromotion amplitude, average thermal phonon number ($\bar{n} \sim 10$) and maximum contrast revival (80%). (d)-(f): Phase space plots and experimental frequency scans at various delays. The circle color represents spin state: black = $|\downarrow\rangle$, white = $|\uparrow\rangle$. (e) and (f) each correspond to single points in (b), as indicated. (d) No momentum kicks; microwave pulses only. (e) Two kicks separated by half a trap period. (f) Two kicks separated by full trap period. (Figure from Ref. [9].)

Quantum Simulations of Magnetism

Trapped atomic ions can be entangled through the application of spin-dependent dipole forces [10, 11]. Conventionally, such forces are applied to subsets of ions in order to execute entangling

quantum gates that are applicable to quantum information processing [1]. When such forces are applied globally, the resulting interacting spin network allows the quantum simulation of a wide variety of spin models such as the Ising and Heisenberg spin chains [12]. The spin-spin interactions originate from modulations of the Coulomb interaction and are therefore long range, and aspects of the system can become classically intractable for even modest numbers of spins $N > 30$. Quantum simulations of magnetism with trapped ions are of particular interest because the interaction graph can be tailored by controlling the external force on the ions, for instance by tuning the spectrum of lasers that provide the dipole force. This allows the control of the sign of the interaction (ferromagnetic vs. antiferromagnetic), the range, the dimensionality, and the introduction of frustration in the system.

Our experiments begin with the ions polarized along an effective magnetic field transverse to long range Ising couplings between the spins [13, 14]. The field is provided by global Raman carrier transitions on all ions, and the Ising couplings arise from an effective Hamiltonian resulting from a virtual coupling through the collective modes of harmonic motion [11]. We operate with the transverse modes of motion in the linear chain [15], so that the modes are tightly packed and all contribute to the effective Ising model. In principle, by controlling the spectrum of light that falls upon each ion in the linear chain, we can program arbitrary fully-connected Ising networks in any dimension [16]. In our current experiments, we use global lasers and a dipole force at a single frequency. However, even with this minimal control we are still able to continuously vary the effective range of the Ising interaction [17]. In practice we can program an Ising interaction that falls off with a power law in distance $1/r^\alpha$, with the exponent between $\alpha = 0.5$ and $\alpha = 1.5$. (Theoretically it should be possible to vary the exponent between $\alpha = 0 - 3$ [18, 17].)

Once in an eigenstate (e.g., the ground state) of the transverse field, we experimentally ramp the field down, and given its final value, we then turn off the interactions and directly measure the state of each spin with a CCD camera. If the field was ramped down adiabatically, we expect the resulting spin order to reflect the properties of the more interesting Ising couplings of the Hamiltonian. For ferromagnetic couplings, we observe a clear phase transition from polarization along the transverse field, and recognize a sharpening in the transition point near the critical magnetic field, as the number of spins is increased [19]. For antiferromagnetic couplings, the gaps are much smaller and the adiabaticity criterion is more stringent. Fig. 2 shows the order seen following a ramp to zero field for $N = 10$ ions, where excited states are clearly created. Of the $2^{10} = 1024$ possible configurations, the two degenerate staggered-order ground states are produced about 18% of the time, with low-lying excitations also prevalent, as shown in the figure. We also observe that as the interaction is made longer range, the creation of excited states is more likely, as the increased level of frustration closes the gap even further and hinders adiabatic evolution. The magnetic field ramp is controlled with a simple radiofrequency modulation source, and we can easily program any type of evolution in time. In addition to using standard exponential and linear ramps, we have also calculated the optimum ramp shape that maintains a constant adiabaticity parameter throughout the evolution, provided through prior knowledge of the many body energy spectrum [20].

By adding an axial field to an antiferromagnetic Ising Hamiltonian, we expect there to be many different orders to emerge as the axial field competes with the Ising couplings. We have been able to directly observe the steps between these orders by lowering the transverse field as before, but to a final state where only the Ising couplings and axial field remain. For N spins, we expect to see $[N/2]$ distinct phases in the ground state, owing to the long-range nature of the Ising interaction. Moreover, as N grows to infinity, the “Devil’s staircase” structure [21] in magnetization becomes a fractal that arises since every rational filling factor (of which there are infinitely many) is a ground state [22].

We have performed quantum simulations with up to $N = 18$ trapped ion spins. While such

quantum simulations can (barely) be predicted classically with under 20 spins, this system holds great promise for the quantum simulation of fully-connected spin chains with 50–100 ions, where many aspects of the system such as dynamical processes become intractable.

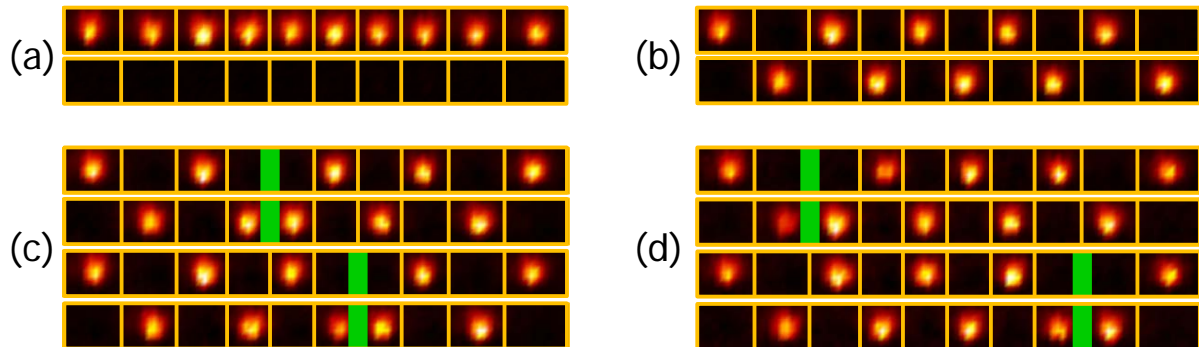


Figure 2. Magnetic ordering of $N = 10$ trapped atomic ion spins with long range antiferromagnetic Ising coupling, conveyed by the spatial images of the crystal having with a length of $22\mu\text{m}$. (a) Reference images of all spins prepared in state $|\uparrow\rangle$ (top) and $|\downarrow\rangle$ (bottom). (b) Ground state staggered order of spins after adiabatically lowering transverse magnetic field. These two degenerate states are produced a total of $\sim 18\%$ of the time. (c) Lowest (coupled) excited states, showing domain walls near the center of the crystal (in green). Any of these four degenerate states are produced a total of $\sim 4\%$ of the time. (d) Next lowest (coupled) excited states, showing domain walls near the ends of the crystal (in green), with these four degenerate states produced a total of $\sim 2\%$ of the time.

Photonic Quantum Networks

Apart from the Coulomb interaction, trapped atomic ions can also be entangled over remote distances through photonic interfaces. Here, an emitted photon from a trapped atomic ion can propagate while carrying entanglement with its host atom, through its polarization, frequency, or longitudinal degrees of freedom [23]. When photons emerging from multiple trapped ions are made to interfere on a beamsplitter, subsequent detection of the photons can herald the entanglement of the trapped ion qubits. While such an interface is necessarily probabilistic, it is not post-selective, and such an interface can be scaled and be made fault-tolerant [24].

There are two common protocols for entanglement of the host ions, involving either one or two photons emitted from the ion pair. In the single photon protocol, each ion is weakly excited, and the beamsplitter erases which path information on which ion emitted the photon, and when the photon is detected on either detector the ions are projected into an entangled state. The excitation is kept weak so that the probability of having two photons is small enough [25]. However, this introduces a fundamental source of error in the entangled state, and moreover this scheme requires interferometric stability of the path lengths to better than an optical wavelength, including the recoiling ions. In the two-photon protocol, the ions are both excited with near unit probability, and the two emitted photons interfere in such a way that only the singlet entangled state of the photons results in their emerging on opposite ports of the beamsplitter [26]. The two photon protocol does not suffer from the shortcomings of the single photon protocols, and for good enough collection probabilities, it will always outperform the single photon protocol. Both protocols can be enhanced by the use of optical cavities to increase the probability of light collection, but this does not change the probabilistic nature of the interface (despite unrealistic proposals to deterministically use photons to entangle ions).

Our early experiments coupling ions to free space admitted a pairwise entanglement rate of about 0.001 Hz [27], limited by the low photon collection probability and also the slow initialization of the ion before each attempt. Current experiments have significantly enhanced

the entanglement rate to approximately 1 Hz, owing to improvements in the particular protocol, initialization, optical light collection, fiber coupling, and detector efficiencies. In the future, the possibility of integrating photonics with ion traps, especially on a semiconductor or silicon chip platform, holds great promise to enhance this rate even further, perhaps by also using optical cavities to further enhance the light collection efficiency [28]. In the end, a juxtaposition of both Coulomb entanglement techniques and photonic entanglement protocols will likely be necessary to scale up the ion trap system [2]. Here, local deterministic operations can be performed within small ion crystals, accompanied by distant-independent probabilistic operations for scaling to very large quantum systems.

Acknowledgments

This work is supported by the U.S. Army Research Office (ARO) Award W911NF0710576 with funds from the DARPA Optical Lattice Emulator Program, ARO award W911NF0410234 with funds from the IARPA MQCO program, ARO award W911NF0910406 with funds from a MURI on Quantum Optical Circuits, and the NSF Physics Frontier Center at JQI.

References

- [1] Wineland D and Blatt R 2008 *Nature* **453** 1008–1014
- [2] Monroe C and Kim J 2013 *Science* **339** 1164
- [3] Olmschenk S, Younge K C, Moehring D L, Matsukevich D N, Maunz P and Monroe C 2007 *Phys. Rev. A* **76** 052314
- [4] Campbell W C, Mizrahi J, Quraishi Q, Senko C, Hayes D, Hucul D, Matsukevich D N, Maunz P and Monroe C 2010 *Phys. Rev. Lett.* **105** 090502
- [5] Hayes D, Matsukevich D N, Maunz P, Hucul D, Quraishi Q, Olmschenk S, Campbell W, Mizrahi J, Senko C and Monroe C 2010 *Phys. Rev. Lett.* **104** 140501
- [6] Liebfried D, Blatt R, Monroe C and Wineland D 2003 *Reviews of Modern Physics* **75** 281
- [7] García-Ripoll, J J, Zoller, P and Cirac J I 2003 *Phys. Rev. Lett.* **91** 157901
- [8] Duan L M 2004 *Phys. Rev. Lett.* **93** 100502
- [9] Mizrahi J, Senko C, Neyenhuis B, Johnson K G, Campbell W C, Conover C W S and Monroe C 2013 *Phys. Rev. Lett.* **110** 203001
- [10] Cirac J I and Zoller P 1995 *Phys. Rev. Lett.* **74** 4091–4094
- [11] Mølmer K and Sørensen A 1999 *Phys. Rev. Lett.* **82** 1835
- [12] Porras D and Cirac J I 2004 *Phys. Rev. Lett.* **92** 207901
- [13] Friedenauer A, Schmitz H, Glueckert J T, Porras D and Schaetz T 2008 *Nature Physics* **4** 757–761
- [14] Kim K, Chang M S, Islam R, Korenblit S, Duan L M and Monroe C 2009 *Phys. Rev. Lett.* **103** 120502
- [15] Zhu S L, Monroe C and Duan L M 2006 *Phys. Rev. Lett.* **97** 050505
- [16] Korenblit S, Kafri D, Campbell W C, Islam R, Edwards E E, Gong Z X, Lin G D, Duan L M, Kim J, Kim K and Monroe C 2012 *New Journal of Physics* **14** 095024
- [17] Islam R, Senko C, Campbell W C, S K, Smith J, Lee A, Edwards E E, Wang C C J, Freericks J K and Monroe C 2013 *Science* **340** 583
- [18] Britton J, Sawyer B, Keith A, Wang C C J, Freericks J, Uys H, Beiruk M and Bollinger J 2012 *Nature* **484** 489–492
- [19] Islam R, Edwards E, Kim K, Korenblit S, Noh C, Carmichael H, Lin G D, Duan L M, Wang C C J, Freericks J and Monroe C 2011 *Nature Communications* **2**:377
- [20] Richerme P, Senko C, Smith J, Lee A, Korenblit S and Monroe C (*Preprint arXiv 1305.2253*)
- [21] Bak P and Bruinsma R 1982 *Phys. Rev. Lett.* **49** 249–251
- [22] Richerme P, Senko C, Korenblit S, Smith J, Lee A, Islam K R, Campbell W C and Monroe C (*Preprint arXiv 1303.6983*)
- [23] Luo L, Hayes D, Manning T A, Matsukevich D N, Maunz P, Olmschenk S, Sterk J D and Monroe C 2009 *Fortschr. Phys.* **57** 1133
- [24] Duan L M and Monroe C 2010 *Reviews of Modern Physics* **82** 1209
- [25] Cabrillo C, Cirac J I, García-Fernández P and Zoller P 1999 *Phys. Rev. A* **59** 1025–1033
- [26] Simon C and Irvine W T M 2003 *Phys. Rev. Lett.* **91** 110405
- [27] Moehring D L, Maunz P, Olmschenk S, Younge K C, Matsukevich D N, Duan L M and Monroe C 2007 *Nature* **449** 68
- [28] Sterk J D, Luo L, Manning T A, Maunz P and Monroe C 2012 *Phys. Rev. A* **85** 062308